

Local electronic structure in MgB_2 from ^{12}B β -NMR

Sylvio Indris* and Paul Heitjans†

Institut für Physikalische Chemie und Elektrochemie, Leibniz Universität Hannover, Callinstraße3-3A, D-30167 Hannover, Germany

Jens Hattendorf and Wolf-Dietrich Zeitz

Hahn-Meitner-Institut, Bereich Strukturforchung, Glienicker Straße 100, D-14109 Berlin, Germany

Thomas Bredow‡

Theoretische Chemie, Leibniz Universität Hannover, Am Kleinen Felde 30, D-30167 Hannover, Germany

(Received 19 June 2006; published 3 January 2007)

We performed β -NMR spectroscopic studies on ^{12}B which was implanted into MgB_2 to get insight into the local electronic structure of this high-temperature superconducting material. By measuring electric field gradients we probed the electronic charge distribution anisotropy around boron in this solid and thus obtained experimental information about the bonding by p electrons. Besides the absolute value, the sign of the electric field gradient was also experimentally determined. By comparison with quantum chemical calculations, some of which were performed in the present work, and with results from conventional NMR spectroscopy on ^{11}B we were able to identify regular boron lattice sites as well as interstitial sites.

DOI: 10.1103/PhysRevB.75.024502

PACS number(s): 74.25.Jb, 61.72.Hh, 71.15.Mb, 76.60.-k

I. INTRODUCTION

Following the discovery of high-temperature oxide superconductors nearly two decades ago¹ the more recent finding that also the simple compound magnesium diboride is a high-temperature superconductor^{2,3} has raised great general interest in the properties of this compound. This extends also to structural properties in the normal conducting state above 39 K, which are the topic of the present paper. MgB_2 consists of alternating hexagonal Mg and B layers (see Fig. 1). The space group is $P6/mmm$ (Ref. 4) with lattice constants $a=3.086$ Å and $c=3.524$ Å². In spite of the simple crystallographic structure of MgB_2 its electronic structure is rather complex with two band gaps leading to anomalous behavior, e.g., of the specific heat.⁵ Band structure calculations have shown that Mg atoms are substantially ionized and that the bands at the Fermi level derive mainly from B orbitals.⁶⁻⁸

Hitherto conventional nuclear magnetic resonance (NMR) studies have been performed on ^{11}B (Refs. 9–13) and ^{25}Mg (Refs. 13–15). We report on the study of MgB_2 by beta-radiation detected NMR (β -NMR)^{16,17} using the β -emitter ^{12}B ($t_{1/2}=20$ ms) as a local probe for the electronic structure. In particular, its quadrupolar interaction was evaluated with the help of multiple quantum transitions (MQT). In this way, the sign of the electric field gradient at a boron site in addition to the absolute value was experimentally determined. MQT were already observed before by β -NMR on polarized, β -active nuclei produced via a nuclear reaction with accelerated ions¹⁸ as well as by thermal neutron capture.¹⁹ In the present work, the former production technique is used. We compare our results on MgB_2 with those from conventional NMR experiments and from our theoretical calculations, presented here as well, in order to get a deeper insight into the local electronic structure and to discriminate between regular and interstitial boron sites. Due to its simple crystal structure

MgB_2 represents an excellent model system, and the comparison between experiment and theory can also be used for testing the quality of quantum chemical calculations. This in turn will help in understanding and predicting the properties of related solid compounds.

II. EXPERIMENT

The MgB_2 powder samples (Alfa Johnson Matthey, 98%) were pressed into pellets with a diameter of 10 mm and a thickness of about 1 mm. The β -NMR experiments were done at the ISL facility at the Hahn-Meitner-Institut, Berlin. A beam of deuteron ions with a kinetic energy of 1.5 MeV was focused onto a boron containing target foil to induce the nuclear reaction $^{11}\text{B}(d,p)^{12}\text{B}$. The target consisted of a thin Al foil onto which a thin layer of B was evaporated. By selection of a recoil angle of 45° the ^{12}B recoil nuclei, which were implanted into the MgB_2 sample, were spin polarized by about 10%.²⁰ ^{12}B is a β emitter with a mean lifetime of 29.4 ms. Since the ^{12}B nuclei are polarized the decay is asymmetric, i.e., more β particles are emitted into the direction of the polarization than opposite to it. The β -radiation asymmetry is defined as

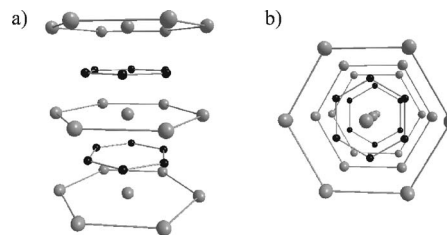


FIG. 1. The planar structure of MgB_2 with hexagonal Mg planes (light grey spheres) and honeycomb B planes (black spheres). (a) View perpendicular to the c axis. (b) View along the c axis.

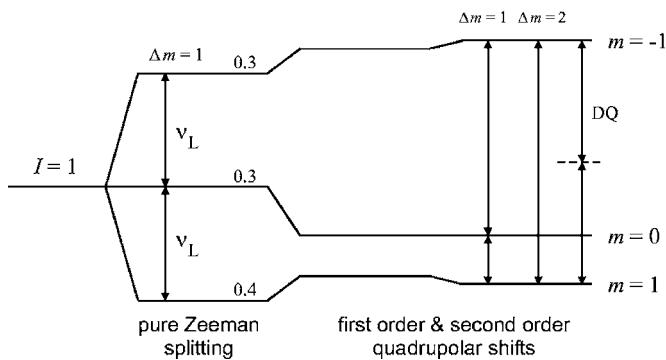


FIG. 2. The energy level diagram for a ^{12}B nucleus ($I=1$) in a magnetic field B and with quadrupolar interaction with an electric field gradient. For strong radiofrequency fields transitions with $\Delta m=2$ and double quantum transitions (DQ) can be excited. The numbers in the left part of the figure give the relative populations of the three energy levels which result from the production process of the ^{12}B nuclei.

$$A_\beta = \frac{Z_N - Z_S}{Z_N + Z_S}, \quad (1)$$

where Z_N and Z_S are the counting rates monitored via two β detectors in the directions north (N) and south (S), respectively, of the external magnetic field.^{16,17}

The polarization of the ^{12}B nuclei can be destroyed by application of a radiofrequency (rf) field with an appropriate frequency. β -NMR spectra consist of the asymmetry A_β recorded as a function of the rf ν . The magnitude of the external magnetic field parallel to the sample polarization is $B = 0.11$ T.

III. SIMULATION OF SPECTRA

^{12}B has a nuclear spin $I=1$ and a nuclear quadrupole moment of $Q = (1.34 \pm 0.14) \times 10^{-30} \text{ m}^2$.²¹ The energy scheme for a ^{12}B nucleus in a magnetic field B and with quadrupolar coupling to an electric field gradient (EFG) is shown in Fig. 2. If the EFG tensor is assumed to have axial symmetry, i.e., $\eta = (V_{xx} - V_{yy})/V_{zz} = 0$, which is reasonable in view of the symmetry of the crystal structure, second order perturbation theory (high field approximation, i.e., $\nu_L \gg \nu_Q$) yields for the energy levels²²

$$E_m = -mh\nu_L + \frac{1}{4}h\nu_Q(3\cos^2\theta - 1) \left[m^2 - \frac{1}{3}I(I+1) \right] - mh \left(\frac{\nu_Q^2}{12\nu_L} \right) \sin^2\theta \left\{ \frac{3}{2}\cos^2\theta [8m^2 - 4I(I+1) + 1] + \frac{3}{8}\sin^2\theta [-2m^2 + 2I(I+1) - 1] \right\}, \quad (2)$$

with the Larmor frequency

$$\nu_L = \frac{\gamma}{2\pi} B \quad (3)$$

and the quadrupole coupling frequency

$$\nu_Q = \frac{3eQV_{zz}}{2I(2I-1)h}. \quad (4)$$

θ is the angle between the direction of the eigenvector corresponding to the maximum (by absolute value) eigenvalue V_{zz} of the electric field gradient tensor and the direction of the magnetic field B , γ is the magnetogyric ratio, e is the elementary charge, Q is the nuclear quadrupole moment, and h is Planck's constant. Due to the symmetry of the crystal structure it is clear that the eigenvector corresponding to V_{zz} is aligned perpendicular to the boron planes and therefore, since $\eta=0$, V_{zz} defines the electric field gradient tensor completely. For $I=1$ the three different states with $m=-1, 0, +1$ belong to the energy levels (see also Fig. 2)

$$\begin{aligned} E_{-1} &= +h\nu_L + \frac{1}{12}h\nu_Q(3\cos^2\theta - 1) \\ &\quad + \frac{\nu_Q^2}{32\nu_L} \sin^2\theta (3\cos^2\theta + 1), \\ E_0 &= -\frac{1}{6}h\nu_Q(3\cos^2\theta - 1), \\ E_{+1} &= -h\nu_L + \frac{1}{12}h\nu_Q(3\cos^2\theta - 1) \\ &\quad - \frac{\nu_Q^2}{32\nu_L} \sin^2\theta (3\cos^2\theta + 1), \end{aligned} \quad (5)$$

and the transition frequencies are

$$\nu_{-1 \leftrightarrow 0} = \nu_L + \frac{1}{4}\nu_Q(3\cos^2\theta - 1) + \frac{\nu_Q^2}{32\nu_L} \sin^2\theta (3\cos^2\theta + 1), \quad (6)$$

$$\nu_{0 \leftrightarrow +1} = \nu_L - \frac{1}{4}\nu_Q(3\cos^2\theta - 1) + \frac{\nu_Q^2}{32\nu_L} \sin^2\theta (3\cos^2\theta + 1), \quad (7)$$

$$\nu_{-1 \leftrightarrow +1} = 2\nu_L + \frac{\nu_Q^2}{16\nu_L} \sin^2\theta (3\cos^2\theta + 1). \quad (8)$$

Whereas $\nu_{-1 \leftrightarrow 0}$ and $\nu_{0 \leftrightarrow +1}$ belong to transitions with $\Delta m=1$, $\nu_{-1 \leftrightarrow +1}$ refers to a transition with $\Delta m=2$. The latter transition can be induced only if electric field gradients are present at the site of the ^{12}B nucleus leading to quadrupolar interaction with the nuclear quadrupole moment and thus to a mixing of the otherwise pure Zeeman states. Furthermore, double quantum transitions are possible (cf. Fig. 2) with a resonance frequency

$$\nu_{\text{DQ}} = \frac{1}{2}\nu_{-1 \leftrightarrow +1}. \quad (9)$$

The populations of the different energy levels, which are also given in Fig. 2, result from the nuclear reaction used to produce the ^{12}B nuclei. Since the upper two levels have the same population, transitions with $m=-1 \leftrightarrow 0$ are not ob-

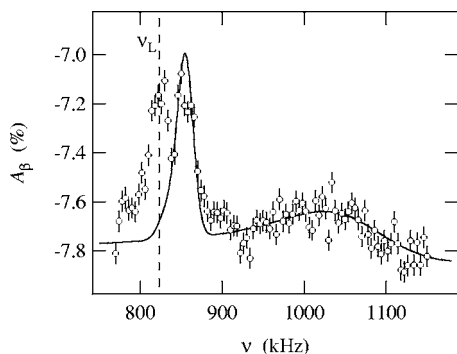


FIG. 3. β -NMR spectrum of ^{12}B in MgB_2 in the range around the Larmor frequency ν_L (corresponding to the magnetic field $B = 0.11$ T) at a temperature of 315 K. The solid line is calculated via Eqs. (7) and (9) using the parameters of the fit shown in Fig. 4.

served in our experiments. This fact can be used to determine not only the absolute value but also the sign of the quadrupole frequency ν_Q and thus of the electric field gradient V_{zz} . For a general discussion of nuclear spin experiments that are feasible to determine the sign of electric field gradients in solids, see Ref. 23.

IV. EXPERIMENTAL RESULTS

Figure 3 shows the ^{12}B β -NMR spectrum of the transition with $\Delta m = 1$ and thus in the region around $\nu_L \approx 823$ kHz for 315 K. Three peaks are visible in the data points. The first one is located around the Larmor frequency, a second one appears at about 30 kHz above ν_L , and a broad, asymmetric peak is located around 1030 kHz. The origin of these three contributions can be identified after considering the transition with $\Delta m = 2$, i.e., the resonance around $2\nu_L$. The corresponding data are displayed in Fig. 4 for a temperature of 303 K.

The resonance for $\Delta m = 2$ shows a broad, slightly asymmetric peak which is shifted from $2\nu_L$ by about 60 kHz, and also a smaller peak around $2\nu_L$. From Eq. (8) it becomes obvious that evaluation of the transition with $\Delta m = 2$ is much easier than for the transition with $\Delta m = 1$ since the terms belonging to first order perturbation theory cancel each other.

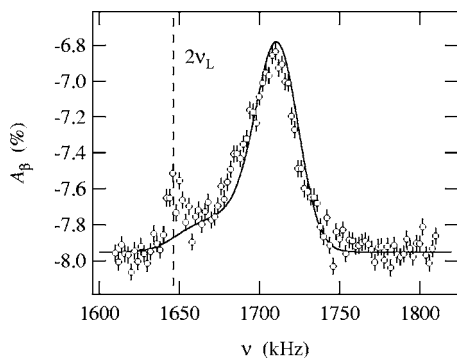


FIG. 4. Resonances of ^{12}B in MgB_2 for $\Delta m = 2$ in the range near $2\nu_L$ at 303 K. The solid line shows the result of a fit using Eq. (8) together with a common powder averaging procedure (Ref. 22).

To describe the experimental line shape we used Eq. (8) together with a common powder averaging procedure (see, e.g., Ref. 22). The resulting fit is shown in Fig. 4 as a solid line and gives the parameters

$$\nu_L = (823 \pm 3) \text{ kHz}, \quad \nu_Q = (853 \pm 38) \text{ kHz}. \quad (10)$$

Since the condition $\nu_L \gg \nu_Q$ is not stringently valid for our system, we verified the results of the second order perturbation theory by comparison with the exact approach (computing the eigenvalues and eigenvectors of the Hamiltonian for the obtained values of ν_L and ν_Q). The difference was smaller than 1%. Using Eq. (4), the value of ν_Q yields an electric field gradient at the ^{12}B site of $V_{zz} = (17.6 \pm 0.8) \text{ V}/\text{\AA}^2$. Comparison with quantum chemical calculations (cf. Sec. V) shows that this peak belongs to ^{12}B atoms which are located at the regular lattice sites in the MgB_2 structure. The additional peak at $2\nu_L$ indicates that some of the ^{12}B atoms are located at sites with a much smaller, though nonvanishing, electric field gradient.

Using the values for ν_L and ν_Q obtained by the fit to the data around $2\nu_L$ shown in Fig. 4 we can identify all contributions to the resonance around ν_L and calculate the solid line shown in Fig. 3. It represents the contributions from the ^{12}B atoms located on regular lattice sites. The broad asymmetric peak at about 1030 kHz originates from transitions with $m = +1 \rightarrow 0$ and is calculated via Eq. (7). From the shift to higher frequencies with respect to ν_L we can determine the sign of the above given field gradient to be positive, i.e., $V_{zz} = +(17.6 \pm 0.8) \text{ V}/\text{\AA}^2$. This corresponds to a “disklike” charge distribution around the ^{12}B nucleus, oriented parallel to the boron planes. The narrow peak at about 855 kHz stems from double-quantum transitions and is calculated via Eq. (9). The frequency where its maximum occurs is half the frequency of the intense maximum in Fig. 4, i.e., of the transition with $\Delta m = 2$, as expected from Fig. 2. The sum of these two contributions gives the solid line shown in Fig. 3. Around ν_L a third contribution is visible which can again be assigned to ^{12}B ions at sites with a small electric field gradient.

Figure 5 shows the temperature dependence of the resonance corresponding to the transition with $\Delta m = 2$ in the range from 348 to 823 K. It reveals that the small peak around $2\nu_L$ broadens with increasing temperature and finally vanishes. In contrast the broad peak at about 1710 kHz increases in intensity and becomes narrower. At 823 K the total line shape can be described by a single Gaussian function. This clearly confirms that the two contributions to the line shape belong to different sites for the implanted boron atoms. The ^{12}B ions are predominantly incorporated at the regular sites in the boron honeycomb layers. At least at low temperatures the ^{12}B nuclei occupy also interstitial sites. The narrowing of the broad peak at high temperatures suggests the onset of boron motion leading to an averaging of the probed electric field gradients.

V. QUANTUM CHEMICAL CALCULATIONS

Electric field gradients (EFG) at the positions of Mg and B atoms of MgB_2 were calculated quantum chemically at the

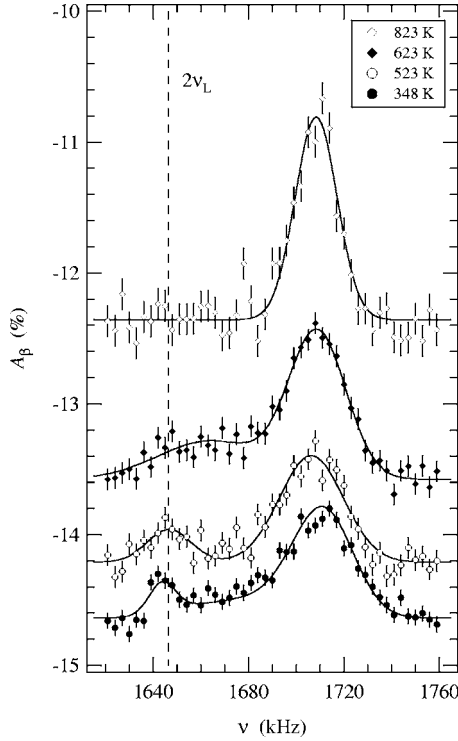


FIG. 5. ^{12}B NMR spectra of MgB_2 in the region around $2\nu_L$ for temperatures between 348 and 823 K.

density-functional level within the generalized-gradient approximation (GGA).²⁴ The Perdew-Wang GGA exchange-correlation functional PW91 was employed as implemented in the crystalline-orbital program CRYSTAL03.²⁵ In this program the Bloch functions are constructed from atom-centered basis functions. In a recent study of the ^7Li EFG in Li_xTiS_2 ,²⁶ it was found that the size of the atomic basis sets has a strong effect on the quality of the calculated results. In

particular d polarization functions at Li atoms were essential to reproduce experimental quadrupole coupling constants. For this reason the available Mg (Ref. 27) and B (Ref. 28) standard basis sets were augmented by two sets of d functions. The basis sets used in the present study are 85-11G(2d) for Mg and 6-21G(2d) for B. Here we followed the standard notation of contracted Gaussian-type basis sets given by Pople and co-workers.²⁹ Inner $1s$ functions of Mg (B) are represented by fixed linear combinations of 8 (6) primitive Gaussian orbitals. A contraction of 5 Gaussians is used to represent the semicore $2s$ and $2p$ functions of Mg. Both valence shells of Mg ($3s$ and $3p$) and B ($2s$ and $2p$) are described at double-zeta level.²⁹

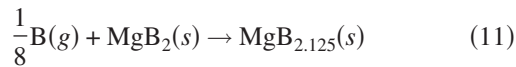
For stoichiometric MgB_2 , the primitive unit cell with experimental lattice constants $a=3.086 \text{ \AA}$ and $c=3.524 \text{ \AA}^2$ was used. The obtained EFG at the regular boron site is $V_{zz} = 14.5 \text{ V/\AA}^2$. Compared with earlier calculations performed with Wien97 (Refs. 7 and 8) this value is smaller but absolute deviations from the experimental results are similar (see Table I). At the Mg positions we get $V_{zz} = -5.5 \text{ V/\AA}^2$ which is larger in absolute value than the measured value 3.07 V/\AA^2 ,¹⁵ and previous theoretical field gradients -2.7 V/\AA (Ref. 27) and -3.2 V/\AA .⁸ In order to investigate the effect of the cell parameters on the calculated EFG, the calculations were repeated with the optimized lattice constants at PW91 level, $a=3.090 \text{ \AA}$, and $c=3.584 \text{ \AA}$. The difference of calculated EFG with experimental and optimized lattice parameters was smaller than 0.1 V/\AA^2 . This could be expected due to the close agreement between theoretical and experimental lattice constants.

Since our experimental results indicate also the presence of ^{12}B nuclei at sites with a much smaller electric field gradient, we also performed calculations for the site in the center of the hexagons of the honeycomb boron layers. We assumed that a single B atom from the foil is implanted into stoichiometric MgB_2 . An Mg_8B_{17} supercell was used to

TABLE I. Comparison of experimental and theoretical results for the electric field gradient V_{zz} at the boron and the magnesium site in MgB_2 . The experimental results are calculated from the quadrupole coupling frequency $\nu_Q = [3eQ/2I(2I-1)\hbar]V_{zz}$ in all cases. I is the nuclear spin and Q is the nuclear quadrupole moment (values for Q taken from Ref. 21). All experiments were done at room temperature.

Method	Nucleus	I	ν_Q in kHz	V_{zz} in V/\AA^2	Citation
β -BMR	^{12}B	1	853 ± 38	$+17.6 \pm 0.8$	This work
NMR	^{11}B	3/2	828 ± 10	16.8 ± 0.2	Gerashenko <i>et al.</i> (Ref. 9)
NMR	^{11}B	3/2	835 ± 5	17.0 ± 0.1	Jung <i>et al.</i> (Ref. 10)
NMR	^{11}B	3/2	836 ± 5	17.0 ± 0.1	Papavassiliou <i>et al.</i> (Ref. 11)
NMR	^{11}B	3/2	845 ± 5	17.0 ± 0.1	Bastow (Ref. 15)
Theory				$+14.53$	This work
				$+18.48$	Hass (Ref. 7)
				$+18.5$	Tsvyashchenko <i>et al.</i> (8)
NMR	^{25}Mg	5/2	222 ± 2	3.05 ± 0.02	Mali <i>et al.</i> (Ref. 14)
NMR	^{25}Mg	5/2	224 ± 20	3.07 ± 0.2	Bastow (Ref. 15).
Theory				-5.5	This work
				-2.7	Haas (Ref. 7)
				-3.2	Tsvyashchenko <i>et al.</i> (Ref. 8)

model this situation, corresponding to the stoichiometry MgB_{2.125}. The cell has one unpaired electron. The doublet ground state was treated with the unrestricted Kohn-Sham method.³⁰ The hypothetical reaction of a gas-phase B atom with MgB₂,



is found to be exothermic. The energy of reaction $\Delta_R E$ is -39 kJ/mol. With the experimental lattice constants of MgB₂ and after full relaxation of all atomic positions we get an electric field gradient of 2.1 V/Å². Thus the field gradient at the interstitial B position is one order of magnitude smaller than at regular B sites which is consistent with our experimental findings. The small field gradient can be explained by the highly symmetric environment of the interstitial site. Since the addition of one B atom is assumed to lead to a lattice expansion, the lattice constants a and c were reoptimized at PW91 level. Surprisingly, the optimized values $a=3.087$ Å and $c=3.666$ Å indicate lattice expansion only in c direction while the length of the cell vectors in the boron plane is essentially unchanged. With the optimized lattice parameters, an EFG of 2.3 V/Å² was obtained at the interstitial B site, similar to the value for the original cell vectors. Therefore lattice relaxation has only a minor effect on the field gradient.

VI. DISCUSSION

The comparison of the experimental spectra with powder-spectra calculations reveals that two different sites are occupied by the ¹²B atoms. One can be assigned to ¹²B atoms sitting on regular B sites and the other one belongs to interstitial ¹²B atoms. This was confirmed by the temperature dependence of the spectra and comparison with quantum chemical calculations. A further way of verification is the comparison with results from conventional NMR on ¹¹B ($I=3/2$) which are summarized in Table I. It shows experimental results for the EFG at the boron site (obtained by β -NMR on ¹²B and conventional NMR on ¹¹B) and the magnesium site (NMR on ²⁵Mg) as well as the results of different quantum chemical calculations (Sec. V, Refs. 10 and 11). Measurements with conventional NMR are not able to yield the sign of the EFG, in contrast to our β -NMR study where we could make use of the strong difference in the populations of the Zeeman levels (cf. Fig. 2). Concerning the boron site, all experimental results for the EFG are equal with respect to the absolute values within the error bars.

Whereas conventional ¹¹B NMR measurements see an average value of the electric field gradient for all boron atoms, and thus predominantly for the boron atoms on regular sites, our measurements are sensitive specifically to the regions around the implanted ¹²B atoms and therefore to structural disorder induced by them.

For all experimental results the EFG was calculated from ν_Q via Eq. (4). One can see that there is good overall agreement between results from conventional NMR and β -NMR as well as between experimental and theoretical results for the electric field gradient. In the case of β -NMR, the latter is true also for the sign of the EFG.

The electric field gradient at the regular boron site in MgB₂ of $V_{zz}=(+17.6\pm 0.8)$ V/Å² is large in comparison to other borides,⁷ where V_{zz} is typically smaller than 7 V/Å². Since the lattice parameters are similar for these borides, this has to be attributed to the fact that the bonding in MgB₂ is based on p electrons only.

To reproduce the experimental spectra a rather broad Gaussian function was necessary for the convolution with the idealized powder spectra. One contribution to the line broadening results from the large rf fields which are necessary to excite these transitions and which lead to the well-known high-power line broadening (see Chap. 11-11 in Ref. 31). Another contribution might be due to the fact that also for boron atoms implanted on regular sites defects or structural disorder in the direct environment may prevail leading to a distribution of electric field gradients.

VII. CONCLUSION

We were able to observe nuclear magnetic resonance transitions of ¹²B in MgB₂ powder samples with $\Delta m=1$ and $\Delta m=2$ by β -NMR spectroscopy. Evaluating the respective frequency regimes around ν_L and $2\nu_L$ gives fully consistent results, in particular for the quadrupole frequency, which allows assignment of all spectral features. Our measurements give access to electric field gradients both at regular boron sites and interstitial sites. Besides the absolute value we also get the sign of the electric field gradient. The assignment to regular and interstitial sites was verified by temperature dependent measurements. The results of quantum-chemical calculations, both from our own work and from the literature, show good agreement with our experimental results.

ACKNOWLEDGMENTS

We are grateful to Hans Ackermann for helpful discussions and constant support over the years.

*Present address: Department of Chemistry, State University of New York at Stony Brook, 100 Nichols Rd., Stony Brook, NY 11794-3400. Electronic address: indris@pci.uni-hannover.de

†Electronic address: heitjans@pci.uni-hannover.de

‡Present address: Institut für Physikalische und Theoretische Che-

mie, Universität Bonn, Wegelerstraße 12, D-53115 Bonn, Germany.

¹J. G. Bednorz and K. A. Müller, Rev. Mod. Phys. **60**, 585 (1988).

²J. Nagamatsu, N. Nakagawa, T. Muranaka, Y. Zenitani, and J. Akimitsu, Nature (London) **410**, 63 (2001).

- ³R. F. Service, *Science* **295**, 786 (2002).
- ⁴M. E. Jones and R. E. Marsh, *J. Am. Chem. Soc.* **76**, 1434 (1954).
- ⁵H. J. Choi, D. Roundy, H. Sun, and M. L. Cohen, *Nature (London)* **418**, 758 (2002).
- ⁶J. Kortus, I. I. Mazin, K. D. Belashchenko, V. P. Antropov, and L. L. Boyer, *Phys. Rev. Lett.* **86**, 4656 (2001).
- ⁷H. Haas, *Hyperfine Interact.* **136/137**, 731 (2001).
- ⁸A. V. Tsvyashchenko, L. N. Formicheva, M. V. Magnitskaya, E. N. Shirani, V. B. Brudanin, D. V. Filosofov, O. I. Kochetov, N. A. Lebedev, A. F. Novgorodov, A. V. Salamatina, N. A. Korolev, A. I. Velichkov, V. V. Timkin, A. P. Menushenkov, A. V. Kuznetsov, V. M. Shabanov, and Z. Z. Akselrod, *Solid State Commun.* **119**, 153 (2001).
- ⁹A. Gerashenko, K. Mikhalev, S. Verkhovskii, T. D'yachkova, A. Tyutyunnik, and V. Zubkov, *Appl. Magn. Reson.* **21**, 157 (2001).
- ¹⁰J. K. Jung, S. H. Baek, F. Borsa, S. L. Bud'ko, G. Lapertot, and P. C. Canfield, *Phys. Rev. B* **64**, 012514 (2001).
- ¹¹G. Papavassiliou, M. Pissas, M. Fardis, M. Karayanni, and C. Christides, *Phys. Rev. B* **65**, 012510 (2002).
- ¹²E. Pavarini, S. H. Baek, B. J. Suh, F. Borsa, S. L. Bud'ko, and P. C. Canfield, *Semicond. Sci. Technol.* **16**, 147 (2003).
- ¹³A. P. Gerashenko, K. N. Mikhalev, S. V. Verkhovskii, A. E. Karikin, and B. N. Goshchitskii, *Phys. Rev. B* **65**, 132506 (2002).
- ¹⁴M. Mali, J. Roos, A. Shengelaya, H. Keller, and K. Conder, *Phys. Rev. B* **65**, 100518(R) (2002).
- ¹⁵T. J. Bastow, *Solid State Commun.* **124**, 269 (2002).
- ¹⁶H. Ackermann, P. Heitjans, and H.-J. Stöckmann, in *Topics in Current Physics—Hyperfine Interactions of Radioactive Nuclei*, edited by J. Christiansen (Springer, Berlin, 1983), Vol. 31, Chap. 6, p. 291.
- ¹⁷P. Heitjans, A. Schirmer, and S. Indris, in *Diffusion in Condensed Matter—Methods, Materials, Models*, edited by P. Heitjans and J. Kärger (Springer, Berlin, 2005), Chap. 9, p. 369.
- ¹⁸R. E. McDonald and T. K. McNab, *Phys. Rev. Lett.* **32**, 1133 (1974).
- ¹⁹D. Dubbers, K. Dörr, H. Ackermann, F. Fujara, H. Grupp, M. Grupp, P. Heitjans, A. Körblein, and H.-J. Stöckmann, *Z. Phys. A* **282**, 243 (1977).
- ²⁰M. Tanaka, S. Ochi, T. Minamisono, A. Mizobuchi, and K. Sugimoto, *Nucl. Phys. A* **263**, 1 (1976).
- ²¹P. Raghavan, *At. Data Nucl. Data Tables* **42**, 189 (1989).
- ²²A. Abragam, *The Principles of Nuclear Magnetism* (Oxford University Press, Oxford, 1999).
- ²³D. Dubbers, H. Ackermann, M. Grupp, P. Heitjans, and H.-J. Stöckmann, *Z. Phys. B* **25**, 363 (1976).
- ²⁴J. P. Perdew and Y. Wang, *Phys. Rev. B* **45**, 13244 (1992).
- ²⁵V. R. Saunders, R. Dovesi, C. Roetti, R. Orlando, C. M. Zicovich-Wilson, and N. M. Harrison, *CRYSTAL03 Users Manual*, University of Torino, Torino, 2003; www.crystal.unito.it
- ²⁶T. Bredow, P. Heitjans, and M. Wilkening, *Phys. Rev. B* **70**, 115111 (2004).
- ²⁷M. I. McCarthy and N. M. Harrison, *Phys. Rev. B* **49**, 8574 (1994).
- ²⁸R. Orlando, R. Dovesi, and C. Roetti, *J. Phys.: Condens. Matter* **2**, 7769 (1990).
- ²⁹W. J. Hehre, R. Ditchfield, and J. A. Pople, *J. Chem. Phys.* **56**, 2257 (1972).
- ³⁰R. G. Parr and W. Yang, *Density-Functional Theory of Atoms and Molecules* (Oxford University Press, New York, 1989).
- ³¹C. P. Poole and H. A. Farach, *Theory of Magnetic Resonance* (John Wiley & Sons, New York, 1987).